RESEARCH ARTICLE

Prediction and Biochemical Demonstration of a Catabolic Pathway for the Osmoprotectant Proline Betaine

Ritesh Kumar,[a] Suwen Zhao,[b] Matthew W. Vetting,[c] B. McKay Wood,[a] Ayano Sakai,[d] Kyuil Cho,[a] José Solbiati,[a] Steven C. Almo,[c] Jonathan V. Sweedler,[a,e] Matthew P. Jacobson,[b] John A. Gerlt,[a,d,e] John E. Cronan[a,d,f]

Institute for Genomic Biology, University of Illinois at Urbana-Champaign, Urbana, Illinois, USA[a]; Department of Pharmaceutical Chemistry, University of California San Francisco, California, USA[b]; Department of Biochemistry, Albert Einstein College of Medicine, Bronx, New York, USA[c]; Department of Biochemistry, University of Illinois at Urbana-Champaign, Urbana, Illinois, USA[d]; Department of Chemistry, University of Illinois at Urbana-Champaign, Urbana, Illinois, USA[e]; Department of Microbiology, University of Illinois at Urbana-Champaign, Urbana, Illinois, USA[f]

ABSTRACT **Through the use of genetic, enzymatic, metabolomic, and structural analyses, we have discovered the catabolic pathway for proline betaine, an osmoprotectant, in *Paracoccus denitrificans* and *Rhodobacter sphaeroides*. Genetic and enzymatic analyses showed that several of the key enzymes of the hydroxyproline betaine degradation pathway also function in proline betaine degradation. Metabolomic analyses detected each of the metabolic intermediates of the pathway. The proline betaine catabolic pathway was repressed by osmotic stress and cold stress, and a regulatory transcription factor was identified. We also report crystal structure complexes of the *P. denitrificans* HpbD hydroxyproline betaine epimerase/proline betaine racemase with L-proline betaine and *cis*-hydroxyproline betaine.**

IMPORTANCE **At least half of the extant protein annotations are incorrect, and the errors propagate as the number of genome sequences increases exponentially. A large-scale, multidisciplinary sequence- and structure-based strategy for functional assignment of bacterial enzymes of unknown function has demonstrated the pathway for catabolism of the osmoprotectant proline betaine.**

Received 31 October 2013 **Accepted** 7 January 2014 **Published** 11 February 2014

Citation Kumar R, Zhao S, Vetting MW, Wood BM, Sakai A, Cho K, Solbiati J, Almo SC, Sweedler JV, Jacobson MP, Gerlt JA, Cronan JE. 2014. Prediction and biochemical demonstration of a catabolic pathway for the osmoprotectant proline betaine. mBio 5(1):e00933-13. doi:10.1128/mBio.00933-13.

Invited Editor Michael Guarnieri, National Renewable Energy Laboratory **Editor** George Drusano, University of Florida

Address correspondence to John E. Cronan, j-cronan@life.uiuc.edu, or John E. Gerlt, j-gerlt@illinois.edu.

Most bacterial habitats are dynamic. The survival and proliferation of bacteria depend upon their ability to adapt to changes in the surrounding environment in such categories as nutrient availability, pH, temperature, and solute concentrations in order to persist and flourish. Hence, bacteria have evolved diverse pathways to overcome unfavorable environmental changes in their microenvironment. Changes in osmolarity are among the more common stresses bacteria encounter, and they respond by accumulating high concentrations of inorganic ions (K^+), amino acids (proline, glutamate), carbohydrates (trehalose, sucrose, glycerol), and/or methylated compounds (glycine betaine, proline betaine [Pro-B], hydroxyproline betaine [Hyp-B], dimethylsulfoniopropionate) (1, 2), often referred to as compatible solutes. Accumulation of compatible solutes has also been reported to counter other environmntal stresses such as cold stress (3, 4).

Betaines are quaternary amine derivatives of amino acids that often serve as osmoprotectants (Pro-B is N,N-dimethylproline and is also called stachydrine). Plants and marine algae are the major producers of Pro-B and are known to accumulate high concentrations of betaines under stress conditions (5–7). Pro-B is excreted from germinating seeds and plant roots into bacterial habitats, and thus, bacteria growing in close association with plants have evolved pathways to utilize betaines for two distinct purposes: as osmoprotectants under high-osmolarity conditions and as carbon and nitrogen sources in the absence of osmotic stress (8–10). Reasonable pathways for Pro-B catabolism have been proposed (9, 11, 12) but have remained without biochemical support.

We previously reported a pathway prediction approach based on genome context plus *in silico* docking of putative substrates in modeled and determined protein structures (13). Put simply, the substrate or product of one enzyme may be the product or substrate of the prior or next enzyme of the pathway. If so, the substrates and products of genome-context-related enzymes should be structurally similar. Consistent results obtained by metabolite docking of several genome-neighborhood-related enzymes allow more-reliable enzyme function predictions. Here, we have built upon this work to delineate the Pro-B catabolic pathway of the soil bacterium *Paracoccus denitrificans* and the aquatic photosynthetic bacterium *Rhodobacter sphaeroides*. Regulation of transcription of the Pro-B catabolic genes triggered by changes in osmotic stress and temperature is reported.

RESULTS AND DISCUSSION

The salient clues to the tHyp-B (*trans*-4-hydroxy-L-proline betaine) degradation pathway determined earlier (13) were the results of *in silico* docking of a metabolite library in the active site of previously determined *Pelagibaca bermudensis* HpbD structure

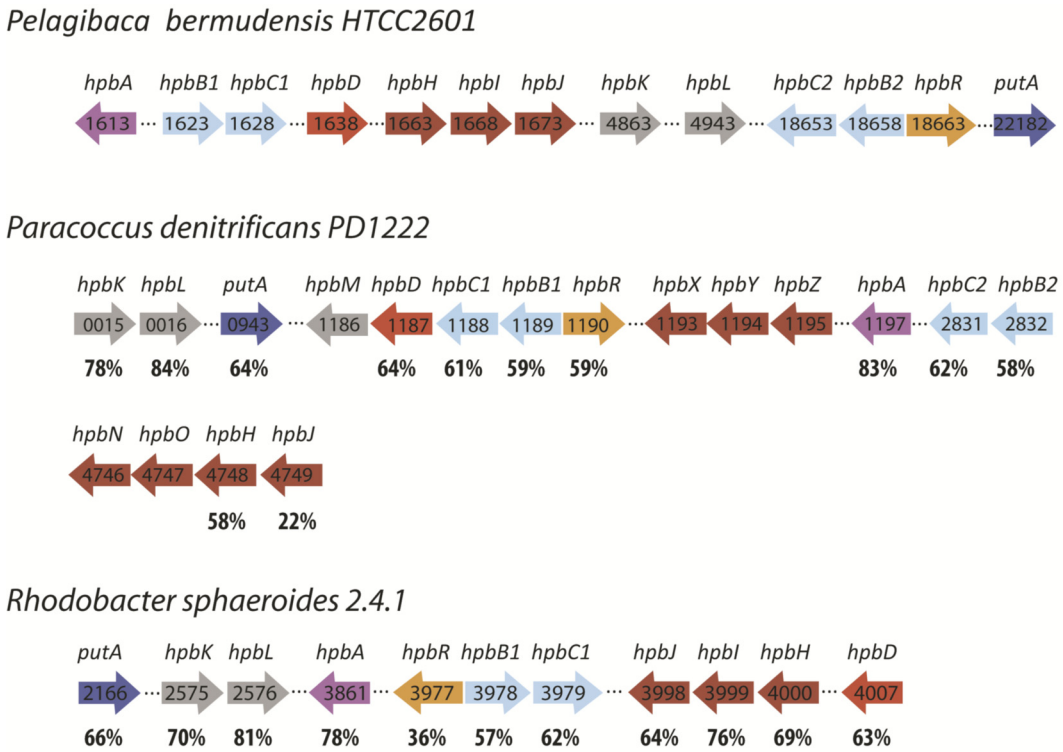

FIG 1 Genome contexts of HpbD in *P. bermudensis* and the orthologous genes in *P. denitrificans* and *R. sphaeroides*. The genes encoding orthologues are given the same color, and the sequence identities relating orthologous genes are indicated. More detail is given in Table S1 in the supplemental material. Genes separated by a string of dots are unlinked in the genome. Note that *in vivo* study of *P. bermudensis* was precluded by its slow growth and very low maximal cell density and by a lack of genetic tools.

plus similar docking of homology models of two proteins, *P. bermudensis* HpbJ (*pb*HpbJ) and *pb*HpbB1, encoded by neighboring genes. These investigations led to the prediction that the substrates of HpbD were the *trans* and *cis* isomers of Hyp-B and/or the L and D forms of Pro-B. HpbD would catalyze the inversion of chirality at Cα and thus perform epimerization on the hydroxyproline derivatives and racemization of the proline derivatives. Indeed, HpbD was found to have activity with both *trans*-Hyp-B and L-Pro-B (13). A *P. denitrificans* protein having sequence (64% identity) and genome context similarities to *P. bermudensis* HpbD (Fig. 1) was also shown to have both activities and thus was named *pd*HpbD. Modeling of *pd*HpbD based on the *P. bermudensis* HpbD crystal structure gave a satisfying model into which Pro-B was readily docked. We have now buttressed this finding by determination of the 2.0-Å crystal structure of unliganded *pd*HpbD and the 1.6-Å and 1.7-Å structures of the complexes of *pd*HpbD with L-Pro-B and with *cis*-Hyp-B, respectively (see Fig. S1 and S2 and Table S1 in the supplemental material). The modeled and determined structures of the L-Pro-B complex with *pd*HpbD agree very well (Fig. 2). A protein from *R. sphaeroides* 2.4.1 encoded in a similar genome context (Fig. 1) was also predicted to contain the same binding site residues (Fig. 2) and thus seemed very likely to catalyze the Pro-B racemase reaction. This was confirmed experimentally (Table 1; see also Fig. S3 in the supplemental material), and the protein was named *rs*HpbD.

***P. denitrificans* utilizes L- and D-Pro-B as carbon and nitrogen sources at low salt concentrations and as osmoprotectants at high salt concentrations.** When grown in minimal media lacking a carbon and/or nitrogen source, *P. denitrificans* and *R. sphaeroides* readily utilized either the L- or D-enantiomers of Pro-B as sole sources of carbon and nitrogen (Fig. 3A). The osmoprotective effects of L- and D-Pro-B were tested under aerobic conditions in minimal medium containing glucose as the carbon source and growth-inhibitory concentrations of NaCl. The L and D forms of Pro-B act as osmoprotectants, although D-Pro-B was the somewhat more efficient osmolyte (Table 2 and Fig. 3B and C), perhaps because it was metabolized more slowly.

Prediction and genetic testing of the Pro-B degradation pathway. We had earlier shown that the proteins and enzymes encoded in the genome neighborhood of HpbD in *P. bermudensis* constitute a catabolic pathway for tHyp-B (13). Based on the reactions catalyzed by members of the families and superfamilies of the proteins encoded within the *hpbD* genome neighborhood (Fig. 1; see also Table S2 in the supplemental material), we predicted a catabolic pathway that degrades L- or D-Pro-B to glutamic acid (Fig. 4). In the case of D-Pro-B, HpbD would catalyze racemization to L-Pro-B. The L-Pro-B would be demethylated to *N*-methyl-L-proline by one or both of the Rieske-type proteins encoded by HpbB1-HpbC1 and HpbB2-HpbC2, and the *N*-methyl-L-proline would be demethylated to L-proline by HpbA, a flavin-dependent enzyme. The pathway would conclude by the action of PutA, a proline dehydrogenase–l-pyrroline-5-carboxylate dehydrogenase. PutA is a bifunctional enzyme that catalyzes two consecutive reactions that oxidize L-proline to L-glutamic acid. Deamination of glutamic acid would give 2-ketoglutarate, the tricarboxylic acid cycle intermediate, and

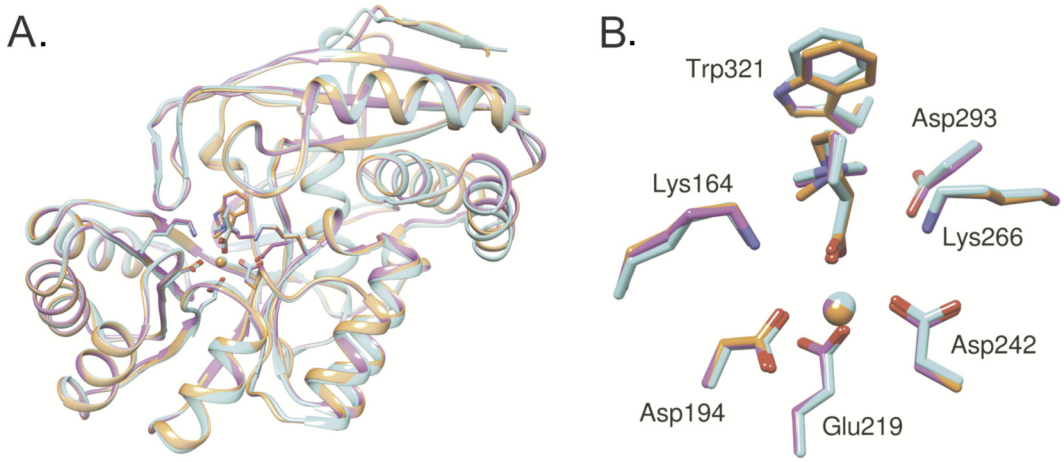

FIG 2 (A) Comparison of two homology models, *pd*HpbD (magenta) and *rs*HpbD (orange), with the X-ray structure of *pd*HpdD (cyan; PDB 4J1O). (B) The Glide XP docking positions of proline betaine in the two models are highly similar to that of the cocrystallized proline betaine of the X-ray structure. Asp194, Glu219, and Asp242 are metal (shown in spheres) binding residues. Lys164 and Lys266 are two catalytic bases, whereas Trp312 and Asp293 are important substrate binding residues.

thereby allow Pro-B to support growth as the sole source of both nitrogen and carbon (Fig. 4).

Another possibility was that the two demethylases could convert D-Pro-B to D-proline, which would be converted to L-proline by a proline racemase and thereby allow D-Pro-B to be used as a carbon and nitrogen source. However, this pathway was rendered unlikely by the finding that neither *P. denitrificans* nor *R. sphaeroides* can grow on D-proline as the sole carbon source (Table 2), although both bacteria utilize D-proline as an osmoprotectant, indicating that D-proline is transported into the cytosol. Hence, these bacteria are probably unable to utilize D-Pro-B due to lack of a proline racemase. This is surprising because it has been reported that 42% of the total free proline in *P. denitrificans* is the D-isomer (14).

To test the hypothesized pathway, strains lacking the racemase were assayed for the ability to grow on the L and D forms of Pro-B as the sole carbon source (Fig. 5A). *hpbD* strain RPd1 lacking the racemase grew well on L-Pro-B but failed to grow on D-Pro-B, whereas the wild-type strain and the *hpbD* strain carrying a plasmid with *hpbD* grew well on both isomers. Identical results were seen for the *hpdD* strain of *R. sphaeroides* (Table 3).

It was recently demonstrated that the *Sinorhizobium meliloti* Rieske protein demethylates L-Pro-B (15). Wild-type growth of strain RPd1 on L-Pro-B suggested that at least one of the two *P. denitrificans* Rieske-type proteins (encoded by *hpbB1* and *hpbC1* or *hpbB2* and *hpbC2*) was responsible for the first demethylation of L-Pro-B. The genes encoding both sets of Rieske-type proteins were separately disrupted to give strains that grew slowly with L- or D-Pro-B as the sole carbon source but had wild-type growth rates with L-proline as the carbon source, suggesting that the two gene sets had redundant functions (Table 2). Hence, a strain was constructed that had disruptions of the genes encoding both Rieske-type proteins. This strain failed to grow on L- or D-Pro-B but showed wild-type growth with N-methyl-L-proline, the product of the first demethylation (Fig. 5B and Table 2). Growth on L- or D-Pro-B was restored upon complementation of the double-mutant strain with *hpbB1* and *hpbC1* expressed on a plasmid from its native promoter (Fig. 5B). Thus, both Rieske-type proteins are demethylases active on L-Pro-B.

The gene encoding the N-methyl L-proline demethylase (*hpbA*) predicted to remove the second Pro-B methyl group was disrupted to give a strain that failed to grow on N-methyl-L-proline or on either Pro-B isomer (Fig. 5C and Table 2). Growth was restored upon complementation with a plasmid expressing the *hpbA* gene from its native promoter (Fig. 5C).

Metabolomics confirms the predicted Pro-B catabolic pathway. The pathway for D-Pro-B degradation (Fig. 4) predicts that Pro-B, N-methyl-Pro, proline, and glutamate should be observed in metabolite extracts of wild-type *P. denitrificans* grown with D-Pro-B as the sole carbon source but not in cells from cultures grown with glucose as the carbon source. Moreover, extracts of a strain fed D-Pro-B that lacked HpbD and both sets of Rieske-type proteins (strain RPd14) should contain only Pro-B and the amino acids normally present, proline and glutamate. (In the feeding experiments, carbon-starved wild-type cells were briefly fed D-Pro-B; see reference 11.) Extracts of these strains were analyzed by liquid chromatography-Fourier transform mass spectrometry (LC-FTMS). The liquid chromatographic retention times of me-

TABLE 1 Kinetic constants of HpbD enzymes of *R. sphaeroides* and *P. denitrificans*

Enzyme and compound	k_{cat} (s^{-1})	K_m (mM)	k_{cat}/K_m (M^{-1} s^{-1})	Source or reference
*rs*HpbD				
L-Pro-B	74 ± 30	440 ± 300	170	This study
D-Pro-B	4.3 ± 0.6	11 ± 4	390	This study
tHyp-B	70 ± 7	16 ± 7	4,300	This study
cHyp-B	58 ± 6	190 ± 30	300	This study
*pd*HpbD				
L-Pro-B	67 ± 10	33 ± 9	2,000	11
D-Pro-B	28 ± 6	7.3 ± 3	3,800	This study

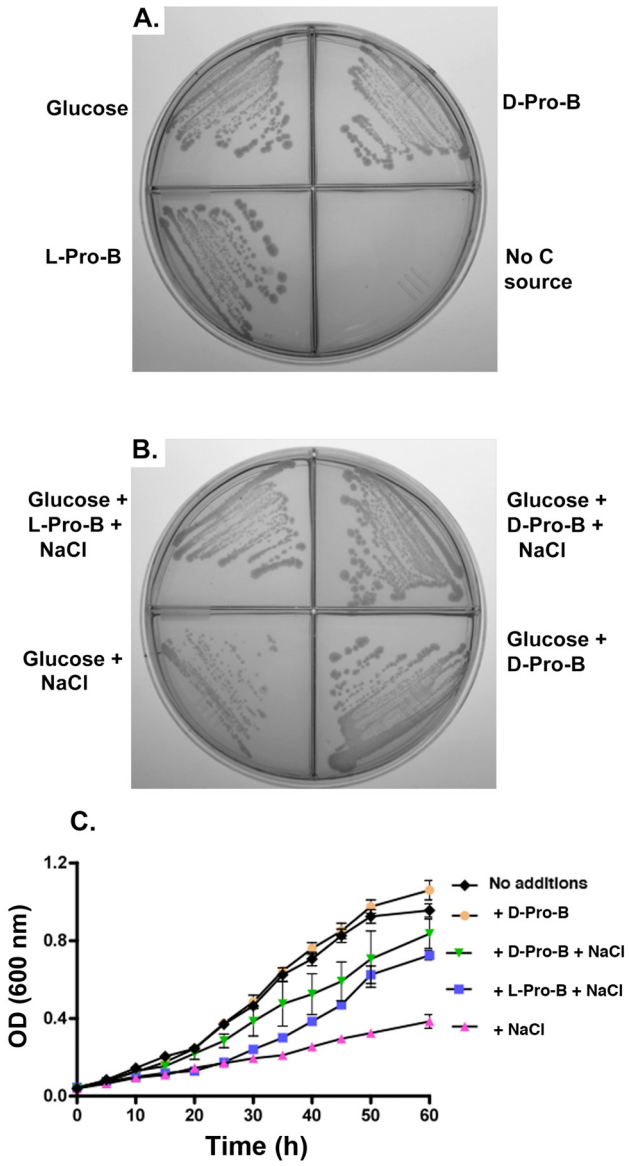

FIG 3 Effects of L- or D-Pro-B on growth of wild-type *P. denitrificans* as the carbon source and as an osmoprotectant. (A) Growth without added NaCl. Growth on glucose is also shown. (B) Growth in the presence or absence of 0.5 M NaCl with or without L- or D-Pro-B supplementation. The L- or D-isomers of ProB were used at a concentration of 20 mM. (C) Effects of addition of the L- or D-isomers of ProB on growth of wild-type *R. sphaeroides* in minimal media containing 0.5 M NaCl. Glucose (20 mM) was present in all cultures.

tabolites from cell extracts were confirmed via accurate mass measurements (± 5 ppm) obtained with the mass spectrometer, and the peaks matched the elution times of Pro-B, proline, and glutamate standards separated by several liquid chromatographic protocols. In extracts of cells grown on D-Pro-B (the wild-type strain) or fed D-Pro-B (mutant strain RPd14), similar Pro-B levels were detected (Fig. 6; see also S5 in the supplemental material). However, only the wild-type cells produced N-methylproline, the product of the first demethylation. The third metabolite in the pathway, proline, was detectable in all samples, but the wild-type cells accumulated nearly 400-fold-more proline than the mutant strain (Fig. 6E). As expected, wild-type cells grown with glucose as the sole carbon source lacked detectable levels of ProB and N-methyl proline but showed proline levels similar to those of the deletion strain fed D-Pro-B. Glutamate, the product of the bifunctional PutA proline dehydrogenase–1-pyrroline-5-carboxylate dehydrogenase, was detected in all three samples (Fig. 6E). An additional metabolomics experiment (not shown) gave intensity patterns similar to those of the D-Pro-B-grown cells. Note that accumulation of D-Pro-B in the mutant strain demonstrated that importation of D-Pro-B is not coupled to its catabolism.

Transcriptional regulation of Pro-B catabolism. In the genomes of *P. bermudensis*, *P. denitrificans*, and *R. sphaeroides*, a gene encoding a LysR homologue (*hpbR*) is found adjacent to the *hpbB1* and *hpbC1* genes that encode a Rieske-type demethylase (Fig. 1). LysR transcription factors comprise one of the largest families of prokaryotic transcriptional regulators and regulate a very diverse range of genes (16). LysR proteins can act as either repressors or activators of transcription upon binding a small-molecule ligand (16, 17). The gene encoding the candidate *P. denitrificans* LysR protein (HpbR) was disrupted to see if it played a role in Pro-B catabolism. The resulting strain (RPd5) showed slow growth with L- or D-Pro-B, but normal growth with L-proline, and thus had a phenotype very similar to that of the strain lacking *hpbB1* and *hpbC1* (Table 2). This result argued that HpbR activates transcription of the neighboring *hpbB1* and *hpbC1* Rieske-type protein genes and perhaps other genes of the Pro-B catabolism pathway. However, the slow growth observed in the absence of HpbR could be due to a high basal level of expression of the target genes or, as in the case of the Rieske demethylases, the presence of another set of genes encoding a duplicate function that does not require HpbR activation.

The most straightforward candidate for the small-molecule ligand of HpbR would be a proline betaine. If so, HpbR was expected to contain the aromatic cage often found in betaine binding sites. Hence, the *P. denitrificans* protein (*pd*HpbR) was modeled on the structure of the *Neisseria meningitidis* CrgA protein (PDB 3HHG). The CrgA protein was chosen based on BLAST analyses using the substrate binding domain of HbpR (residues 98 to 291) as the query plus its crystal structure. Although another sequence gave a slightly better sequence match, it was an inferior template because its crystal structure (PDB 2QSX) contains two disordered segments. Although the overall amino acid sequence identity between *pd*HpbR and CrgA is relatively low (21%), the modeled *pd*HpbR ligand binding site residues Tyr147, Trp200, and Trp242 form an aromatic cage capable of the cation-π interactions used in betaine binding. Two residues, Asp163 and Arg194, that could act to shape the binding site electric field are also present. This homology model was used for induced-fit docking with Pro-B as the ligand (see Fig. S4 in the supplemental material). In the liganded model, the quaternary ammonium of the ligand fits well into the aromatic cage, whereas Arg194 forms salt bridges with the carboxylate group of the ligand and Asp163 interacts with the positively charged quaternary ammonium group. The HpbR proteins of *P. bermudensis* and *R. sphaeroides* were also modeled, and these proteins also formed potential aromatic cage structures (see Fig. S4).

Pro-B induces increased transcription of the genes of the pathway. To investigate the role of Pro-B and HpbR in expression of the *P. denitrificans* and *R. sphaeroides* Pro-B degradation genes, cultures of the wild-type strains were grown with sole carbon

TABLE 2 Growth phenotypes of *P. denitrificans* amd *R. sphaeroides* wild-type and mutant strains[a]

Genotype	Strain	Phenotype					
		Glucose	Succinate	L-Pro-B	D-Pro-B	L-Pro	N-methyl-L-Pro
Wild type	PD1222	+++	+++	+++	+++	+++	++
hpbD	RPd1	+++	+++	+++	−	+++	++
shpbB1 hpbC1	RPd2	+++	+++	++	++	+++	++
shpbB2 hpbC2	RPd3	+++	+++	++	++	+++	++
hpbB1 hpbC1 and *hpbB2 hpbC2*	RPd4	+++	+++	−	−	+++	++
hpbR	RPd5	+++	+++	++	++	+++	++
hpbA	RPd6	+++	+++	−	−	+++	−
RPd1 complemented with *hpbD*	RPd10	+++	+++	+++	+++	+++	++
RPd2 complemented with *hpbB1* and *hpbC1*	RPd11	+++	+++	+++	+++	+++	++
RPd6 complemented with *hpbA*	RPd12	+++	+++	+++	+++	+++	++
putA	RPd13	+++	+++	−	−	−	−
	2.4.1	+++	+++	++	++	+++	+
hpbD	RRs1	+++	+++	+++	−	+++	++

[a] +++, growth similar to that of the wild-type strain (note that none of the strains grew on D-proline); ++ and +, slow-growth phenotypes, −, growth-defective phenotype. Assays were performed in triplicate (from five separate cultures).

sources of glucose, L-proline, or L- or D-Pro-B in minimal medium, and quantitative reverse transcription-PCR (qRT-PCR) transcriptional analyses were performed. Relative to glucose-grown cells, transcription of the racemase gene, *hpbD*, and the genes encoding all demethylase proteins was increased 8- to 15-fold in cells grown on either L- or D-proline. In contrast, the expression levels of L-proline-grown cells did not significantly differ from those of glucose-grown cells (Table 3). Transcription of several genome-proximal genes encoding putative transport proteins also increased in Pro-B-grown cells, but L-proline-grown cells also showed increased transcription. The putative transport genes had lower induction ratios than the catabolic enzyme genes as expected from a high basal level of inducer transport required to initiate induction (Table 3).

Pro-B induction also demonstrated hallmarks of secondary regulatory interactions. Expression of the gene encoding PutA, the enzyme that converts L-proline to glutamate, increased in Pro-B-grown cells, presumably due to accumulation of L-proline (cells grown on L-proline showed similarly increased *putA* transcription). Demethylation of Pro-B results in the synthesis of formaldehyde, a toxic compound, and thus bacteria that utilize Pro-B as the carbon source should have a pathway to neutralize formaldehyde. It has been reported that *P. denitrificans* can utilize methanol as a carbon source (18), which involves formation of formaldehyde, and thus the bacterium has an efficient formaldehyde detoxification pathway. The detoxification pathway is induced by formaldehyde and includes a glutathione-dependent formaldehyde dehydrogenase (*hpbK*) and an S-formylglutathione hydrolase (*hpbL*). Both genes showed a 20-fold increase in transcript levels in cultures grown on Pro-B, consistent with formaldehyde formation as a product of Pro-B catabolism (Table 3). The *hpbM* gene, which encodes a GroES domain alcohol dehydrogenase with sequence similarity to formaldehyde dehydrogenase, showed a 5-fold upregulation in cells grown on Pro-B, suggesting a possible role in formaldehyde detoxification (Table 3). However, no increase in *hpbM* transcript levels was observed when cells were grown with methanol, suggesting that its expression is regulated by Pro-B but not by formaldehyde.

Expression of the genes encoding the *P. denitrificans* HbpR LysR-type transcription factors was unaffected by growth on Pro-B (Table 3). However, disruption of the *P. denitrificans hpbR* gene severely decreased induction of the Pro-B catabolic genes, consistent with previously discussed evidence that HpbR is a key transcriptional activator that modulates response to Pro-B (Table 3).

A similar but less extensive set of qRT-PCR analyses were performed with the *R. sphaeroides* wild-type strain (Table 4). The data were very similar to those obtained with *P. denitrificans.*

Salt stress and cold stress suppress the Pro-B catabolic pathway. This work has been mainly concerned with Pro-B as a carbon and nitrogen source. However, under osmotic stress conditions Pro-B catabolism must be largely suppressed to allow a high intracellular concentration of the osmolyte to accumulate in the bacterial cytosol. Moreover, Pro-B transport should increase to aid osmolyte accumulation. In accord with these predictions, in cultures of wild-type strains of *P. denitrificans* and *R. sphaeroides* grown on glucose in media containing 0.5 M NaCl, expression of the catabolic genes was severely repressed relative to that seen with cultures grown without added NaCl (Tables 3 and 4). Use of D-Pro-B as the carbon source in 0.5 M NaCl resulted in less repression of the catabolic genes, although the expression levels remained well below those seen in the same medium lacking added NaCl. In contrast, NaCl addition did not suppress transcription of the genes encoding the putative transport proteins and, in the case of the *hpbX hpbY hpbZ* gene cluster, salt stress gave increased transcription consistent with accumulation of the osmolyte. Therefore, salt stress suppresses expression of the catabolic pathway genes but not of the transport genes and thereby allows Pro-B to accumulate and function as an osmoprotectant.

Although this scenario fits the terrestrial bacteria *P. denitrificans* and *R. sphaeroides*, the Pro-B degradation pathway was first identified in *P. bermudensis*, a marine bacterium. *P. bermudensis* was isolated from the open ocean (the Sargasso Sea) where salt concentration and hence osmolarity are essentially invariant. Hence, although *P. bermudensis* could take nutritional advantage of Pro-B produced by marine algae, the compound would likely not be used to counter osmotic stress. This raised the issue of the relevance of Pro-B accumulation for this bacterium. However, in

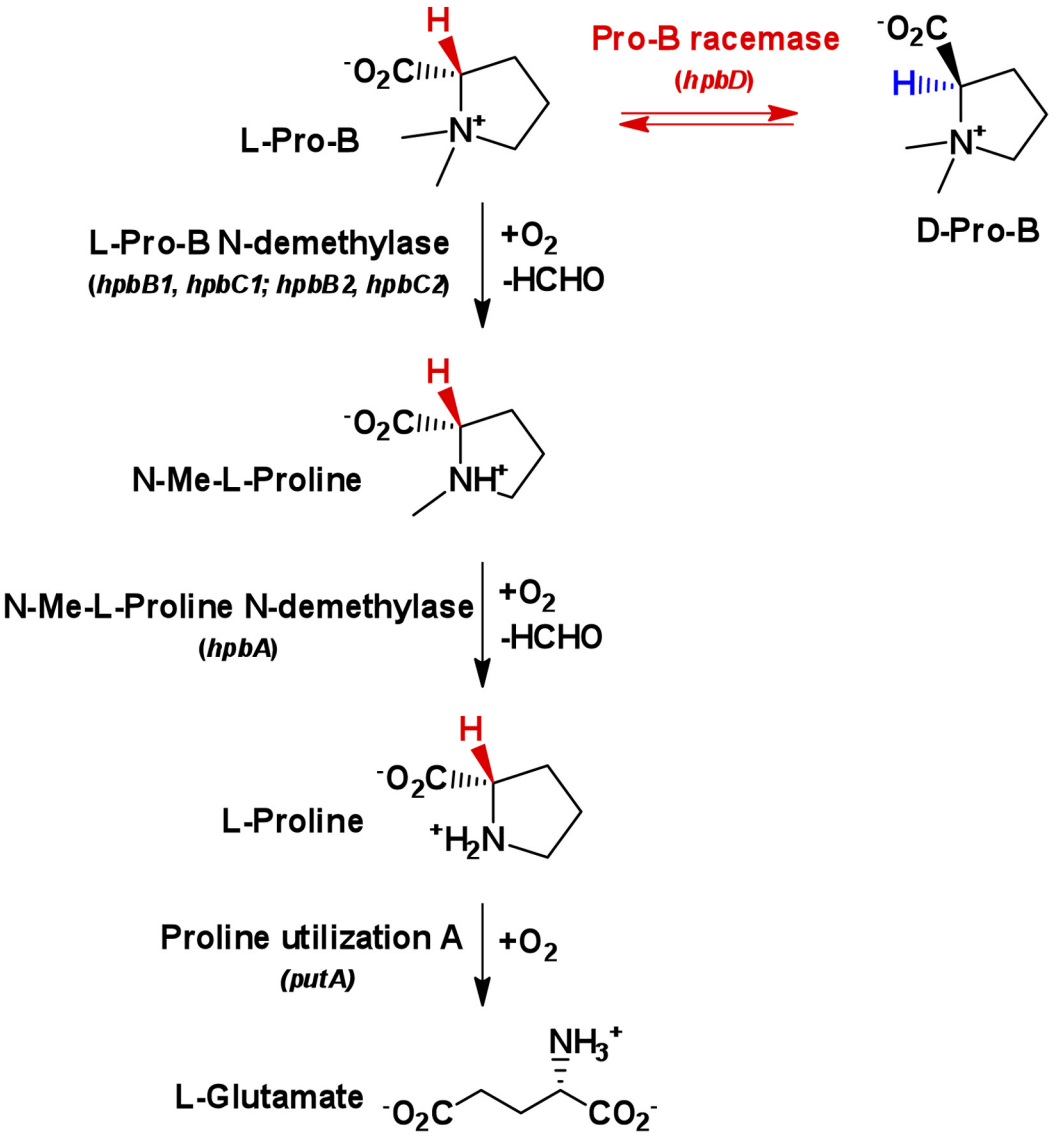

FIG 4 Proposed pathway for L-Pro-B and D-Pro-B catabolism based on the genome neighborhood contexts in *P. bermudensis*, *P. denitrificans*, and *R. sphaeroides*. The interconversion of L-Pro-B and D-Pro-B is catalyzed by HpbD; L-Pro-B undergoes two N demethylations to L-Pro; and finally, L-Pro oxidation is catalyzed by a bifunctional enzyme PutA to give L-glutamate, which is readily deaminated to ammonia plus 2-ketoglutarate, the citric acid cycle intermediate.

Bacillus subtilis and *Listeria monocytogenes*, betaines have been reported to play a significant role in cold tolerance (3, 4). Since marine bacteria experience temperature fluctuations upon depth changes, *P. dentrificans* and *R. sphaeroides* were tested to see if these bacteria respond to low temperature in a manner similar to the high-salt response. Indeed, in both bacteria, expression of the Pro-B catabolism genes in 15°C-grown cultures was significantly lower than in 30°C-grown cultures (Tables 2 and 4). Given these results, L-Pro-B supplementation would be expected to give increased growth of *P. dentrificans* at 15°C, but not at 30°C, and this was the case (Fig. 7).

These results strongly suggest that plants and marine algae make the D enantiomer of Pro-B as well as the L enantiomer because of the conservation of HpbD in plant- and alga-associated bacteria and its coregulation with the enzymes of L-Pro-B catabolism. However, in several literature searches, no reports in which the enantiomer composition of Pro-B isolated from nature has been assayed were found.

All extant sequenced bacterial genomes were analyzed for the presence of genes encoding putative Pro-B metabolism proteins having more than 50% sequence similarity with the respective proteins of *P. denitrificans*. This gave a list of about 100 bacterial species (see Table S4 in the supplemental material). Interestingly, 47% of the candidates are plant-associated bacterial species, 20% are marine bacteria that share a microenvironment with marine macroalgae, and another 8% are soil bacteria known to live in close proximity with plants.

In the present study, the Pro-B catabolic pathway of *P. denitri-*

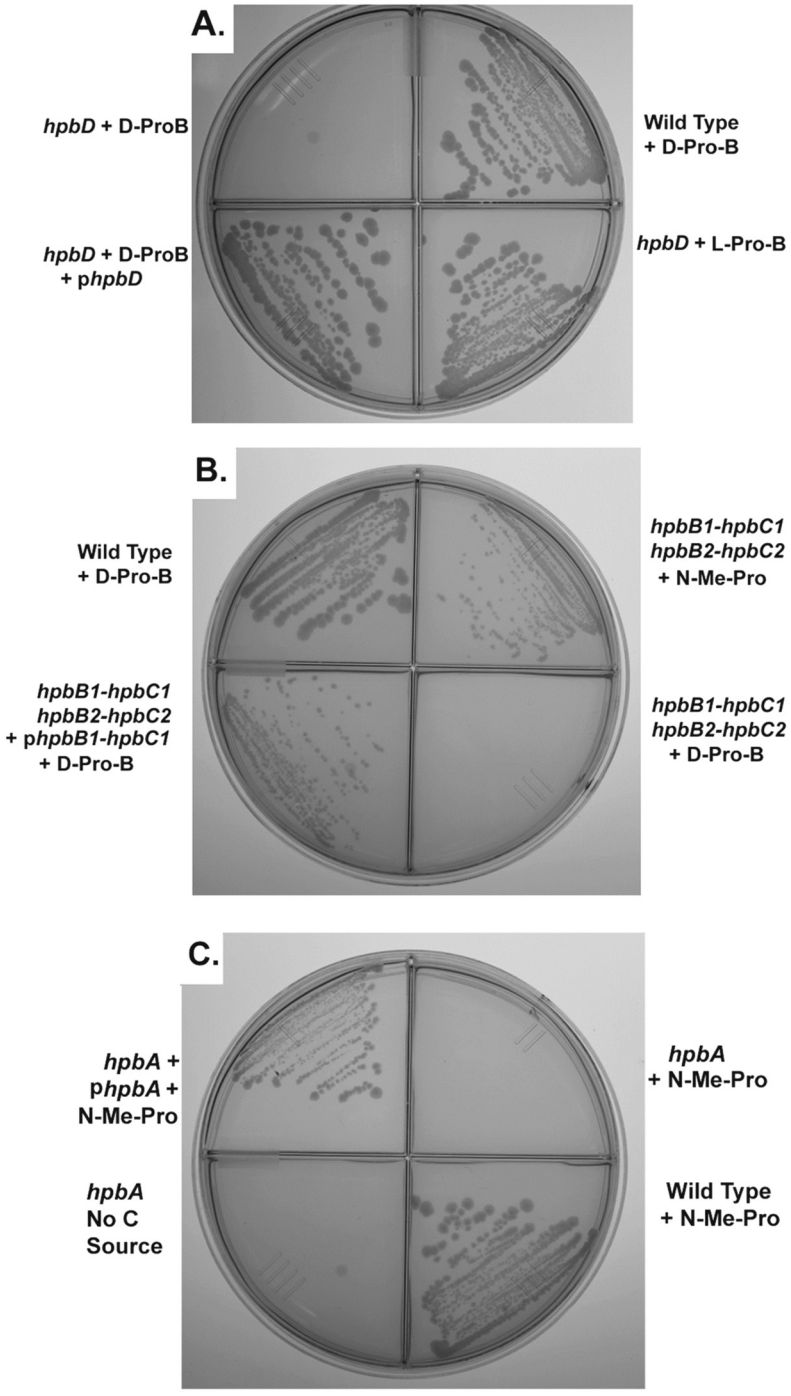

FIG 5 Growth phenotypes. (A) Growth of the *P. denitrificans* wild-type strain (Pd1222) or mutant strains (RPd1 and RPd10) in minimal medium with L- or D-Pro-B. The h*pbD* strain was RPd1, and the complemented strain was RPd10. (B) Growth of the *P. denitrificans* wild-type strain (Pd1222) or mutant strains (RPd4 and RPd11) in minimal medium with D-Pro-B or N-Me-Pro. The strain missing both Rieske demethylases (genes *hpbB1* and *hpbC1* and genes *hpbB2* and *hpbC2*) was RPd4, and the complemented strain was RPd11. (C) Growth on N-Me-Pro as the carbon source. The *P. denitrificans hpbA* strain was RPd6, and the complemented strain was RPd12.

ficans and *R. sphaeroides* has been demonstrated. We propose that pathway docking in combination with computational biology, enzymology, metabolomics, and microbiology provides a powerful tool for identification and subsequent experimental verification of novel pathways in diverse bacteria.

MATERIALS AND METHODS

Homology modeling and docking. The models of *pb*HpbD, *rs*HpbD, and *pd*HpbR were built using our in-house software Protein Local Optimization (PLOP; marketed as Prime by Schrödinger LLC) v 25.0. The PDB template used for the two HpbD enzymes is 2PMQ and for *pd*HpbR is 3HHG. The sequence alignment of each pair of target and template was made using the L-INS-i method in MAFFT v 7.012b (19). Proline betaine was docked to the three models, and its three-dimensional (3D) conformation was prepared by LigPrep (20). Two docking methods were used. The Glide XP (21) docking method was used on two HpbD models; the details have been described previously. Induced-fit docking (22) was used on *pd*HpbR, which allowed side chains within 10 Å of the ligand to be flexible, and Glide XP was used for redocking.

Cloning and expression of *P. denitrificans hpbD*. The *P. denitrificans hpbD* gene was amplified from the genomic DNA using primers PD1187F and PD1187R (see Table S2 in the supplemental material). PCR was performed using KOD Hot Start DNA polymerase (Novagen). The conditions were 2 min at 95°C, followed by 40 cycles of 30 s at 95°C, 30 s at 66°C, and 30 s at 72°C. The amplified fragments were cloned into an N-terminal tobacco etch virus (TEV)-cleavable StrepII-6×His tag-containing vector, pSGC, by ligation-independent cloning (23). All growth media contained 100 μg/ml kanamycin sulfate and 35 μg/ml chloramphenicol. Plasmid was transformed into *Escherichia coli* Rosetta2(DE3) pLysS (Novagen) and plated on Luria-Bertani (LB) agar plates. Five to 10 colonies were used to inoculate 100 ml of LB media and allowed to grow overnight at 37°C (250-rpm agitation). The overnight cultures were used to inoculate 4 liters of autoinduction media in 10 2-liter flasks and incubated (250-rpm agitation) at 25°C for 24 h, reaching an optical density at 600 nm (OD_{600}) of 20 to 25 (24, 25). The cells were harvested by centrifugation and stored at −80°C.

Purification of *pd*HpbD. All purification steps were performed at 4°C. Cells were resuspended (4:1 [vol/wt]) in buffer A {50 mM 2-[4-(2-hydroxyethyl)piperazine-1-yl] ethanesulfonic acid [pH 7.8], 150 mM NaCl, 10% glycerol, 20 mM imidazole} with 0.1% Tween 20 and then disrupted by sonication. The cellular extract was clarified by centrifugation at 4°C and applied to a 10-ml nickel (Ni)-Sepharose HP (GE Healthcare) column. The column was washed with 10 column volumes of buffer A, and proteins were step eluted with 300 mM imidazole–buffer A. TEV protease (1/50 [wt/wt]) was added to the pooled protein-containing fractions, and the reaction was dialyzed overnight against

TABLE 3 Transcriptional analysis by qRT-PCR of wild-type *P. denitrificans* (strain PD1222) and *P. denitrificans htpR* strain RPd5[a]

Strain and gene	Locus tag (Pden)	Fold change in gene expression						
		L-Pro	L-Pro-B	D-Pro-B	Glucose (0.5 M NaCl)	D-Pro-B (0.5 M NaCl)	Methanol	15°C
P. denitrificans wild type								
Racemase								
hpbD	1187	1.1 ± 0.2*	9 ± 1.5	11 ± 1.5	−7 ± 1.0	3 ± 0.5	—	−2.5 ± 0.5
Demethylases								
hpbC1	1188	1.1 ± 0.2*	14 ± 2.0	13 ± 1.5	−8 ± 1.0	2.1 ± 0.5	—	−2.3 ± 0.3
hpbB1	1189	1.5 ± 0.1*	15 ± 0.9	13 ± 0.5	−5 ± 0.4	2.8 ± 0.4	—	−2.7 ± 0.3
hpbC2	2831	1.1 ± 0.3*	7.7 ± 0.5	9.2 ± 0.5	−7 ± 0.3	2.7 ± 0.4	—	3.1 ± 0.5
hpbB2	2832	1.3 ± 0.2*	7.8 ± 0.6	10 ± 0.7	−6 ± 0.5	2.2 ± 0.3	—	−3.6 ± 0.4
hpbA	1197	1.5 ± 0.2	12 ± 1.1	12 ± 0.8	−5 ± 0.7	2.7 ± 0.2	—	−2.7 ± 0.5
Transcription factor								
hpbR	1190	1.5 ± 0.1*	1.9 ± 0.1*	1.1 ± 0.1*	1.1 ± 0.1*	1.0 ± 0.2*	—	—
Putative transporters								
hpbX	1193	2.9 ± 0.2	3.9 ± 0.3	3.5 ± 0.7	8.5 ± 1.0	4.5 ± 0.2	—	—
hpbY	1194	2.2 ± 0.2	3.5 ± 0.5	4.2 ± 0.4	9.5 ± 0.6	5.5 ± 0.5	—	—
hpbZ	1195	2.1 ± 0.1	2.5 ± 0.4	4.4 ± 0.4	10.5 ± 0.5	4.5 ± 0.3	—	—
hpbJ	4749	2.5 ± 0.3	6.5 ± 1.6	7.2 ± 1.5	5.2 ± 0.3	10 ± 0.6	—	—
hpbH	4748	2.4 ± 0.3	7.1 ± 1.5	6.9 ± 1.3	4.3 ± 0.5	14 ± 1.2	—	—
hpbO	4747	2.3 ± 0.3	5.5 ± 0.7	6.5 ± 0.5	4.9 ± 0.4	15.5 ± 0.9	—	—
hpbN	4746	2.5 ± 0.2	5.5 ± 1.0	7.5 ± 1.4	4.2 ± 0.5	12.5 ± 1.3	—	—
Proline catabolism								
putA	94	4.2 ± 0.4	3.1 ± 0.5	3.5 ± 0.5	1.0 ± 0.1*	2.5 ± 0.3	—	—
hpbM	1186	1.5 ± 0.2*	4.9 ± 0.5	4.5 ± 0.4	−1.1 ± 0.3*	2.5 ± 0.2*	4.5 ± 0.5	—
Formaldehyde detoxification								
hpbK	15	1.1 ± 0.1*	22 ± 2.5	19.5 ± 3	1.1 ± 0.1*	6.0 ± 1.0	25 ± 3	—
hpbL	16	1.3 ± 0.2*	21 ± 3.5	19.8 ± 2	−1.5 ± 0.1*	7.5 ± 2.0	28 ± 2	—
P. denitrificans hpbR								
Racemase								
hpbD	1187	1.1 ± 0.2*	3 ± 0.5	5.0 ± 1.1	−7.5 ± 1.0	3.5 ± 0.5	—	—
Demethylases								
hpbC1	1188	1.2 ± 0.2*	3.4 ± 2.0	2.3 ± 0.5	−8.5 ± 1.0	2.5 ± 0.5	—	—
hpbB1	1189	1.4 ± 0.1*	2.2 ± 0.9	2.2 ± 0.3	−6.7 ± 0.4	2.4 ± 0.3	—	—
hpbC2	2831	1.1 ± 0.2*	2.1 ± 0.5	2.2 ± 0.5	−7.1 ± 0.5	3.7 ± 0.2	—	—
hpbB2	2832	1.4 ± 0.1*	2.3 ± 0.6	2.1 ± 0.5	−6.8 ± 0.5	3.2 ± 0.3	—	—

[a] The strains were cultured in minimal medium containing 20 mM glucose or succinate as the sole carbon source, and gene expression was compared to that of the strain grown in minimal media on different carbon sources (L-Pro-B, D-pro-B, L-proline, methanol, or glucose supplemented with 0.5 M NaCl) at either 30°C or 15°C. The identity of each gene is indicated by the genome locus name. Assays were performed in triplicate (four biological replicates), and the data are averages and standard deviations of the results. The average ratio is the fold difference compared to cells grown with glucose as a carbon source. *P* value < 0.005. The qRT-PCR analyses were done as described in Materials and Methods. *, not significant; —, not determined.

buffer A with 300 mM imidazole. The pooled eluate was then concentrated to 15 to 30 mg/ml and applied to a 16/60 Superdex 200 column (GE Healthcare) equilibrated against buffer B {10 mM 2-[4-(2-hydroxyethyl)piperazine-1-yl] ethanesulfonic acid (pH 7.8), 150 mM NaCl, 5% glycerol, 1 mM EDTA, 1 mM dithiothreitol (DTT)}. Fractions with >95% purity by SDS-PAGE were pooled and concentrated to 15 to 30 mg/ml by centrifugal ultrafiltration. Aliquots were snap-frozen in liquid nitrogen and stored at −80° C

Crystallization and structure solution of *pd*HpbD. Crystals were obtained by vapor diffusion at 18°C using the sitting drop vapor diffusion method in 96-well IntelliPlates (Art Robbins). Equal volumes of protein (27.5 mg/ml in 10 mM HEPES [pH 7.5], 150 mM NaCl, 5% [wt/vol] glycerol, 1 mM EDTA, 1 mM DTT) and crystallization buffer (30% [vol/vol] polyethylene glycol 400 [PEG 400], 0.1 M MES [morpholineethanesulfonic acid] [pH 6.5], 200 mM $MgCl_2$) were combined and equilibrated against 70 μl of crystallization buffer in the reservoir. Crystals were soaked for 5 min in the reservoir solution for unliganded structures or in the reservoir solution supplemented with 200 mM L-proline betaine or 200 mM tHyp-B (*trans*-4-hydroxy-L-proline betaine) for the complexes. Crystals were flash cooled by immersion in liquid nitrogen and subsequently stored and shipped to Advanced Photon Source beamline 31-ID (Lilly-CAT). Data were collected at 100 K and a wavelength of 0.97929 Å. Data were processed using MOSFLM (26) and scaled in space group $P42_12$ using SCALA (27). A monomer from a related proline betaine racemase (J. B. Bonanno, M. Rutter, K. T. Bain, C. Lau, V. Sridhar, D. Smith, S. Wasserman, J. M. Sauder, S. K. Burley, S. C. Almo, New York SGX Research Center for Structural Genomics [NYSGXRC]; PDB 2PMQ) was used as a search model in molecular replacement. PHASER (28), within the refinement package PHENIX (29), located two subunits which by crystallographic symmetry generated the expected molecular octamer. Several rounds of manual rebuilding and ligand and water fitting within the molecular graphics program COOT (30) followed by refinement in PHENIX were performed to finalize the structure. Iodine atoms, originating from the preparations of Pro-B and tHyp-B, were modeled into difference density peaks with features suggestive of bound iodine. The geometry restraints for the ligands were produced using ELBOW within PHENIX. L-Pro-B (substrate) and *cis*-4OH–D-proline betaine (cHyp-B [product]) were chosen as the modeled ligands in the respective complexes based on the fit to the electron density; however, the liganded structures are presumed to be a racemic mixture due to turnover in the

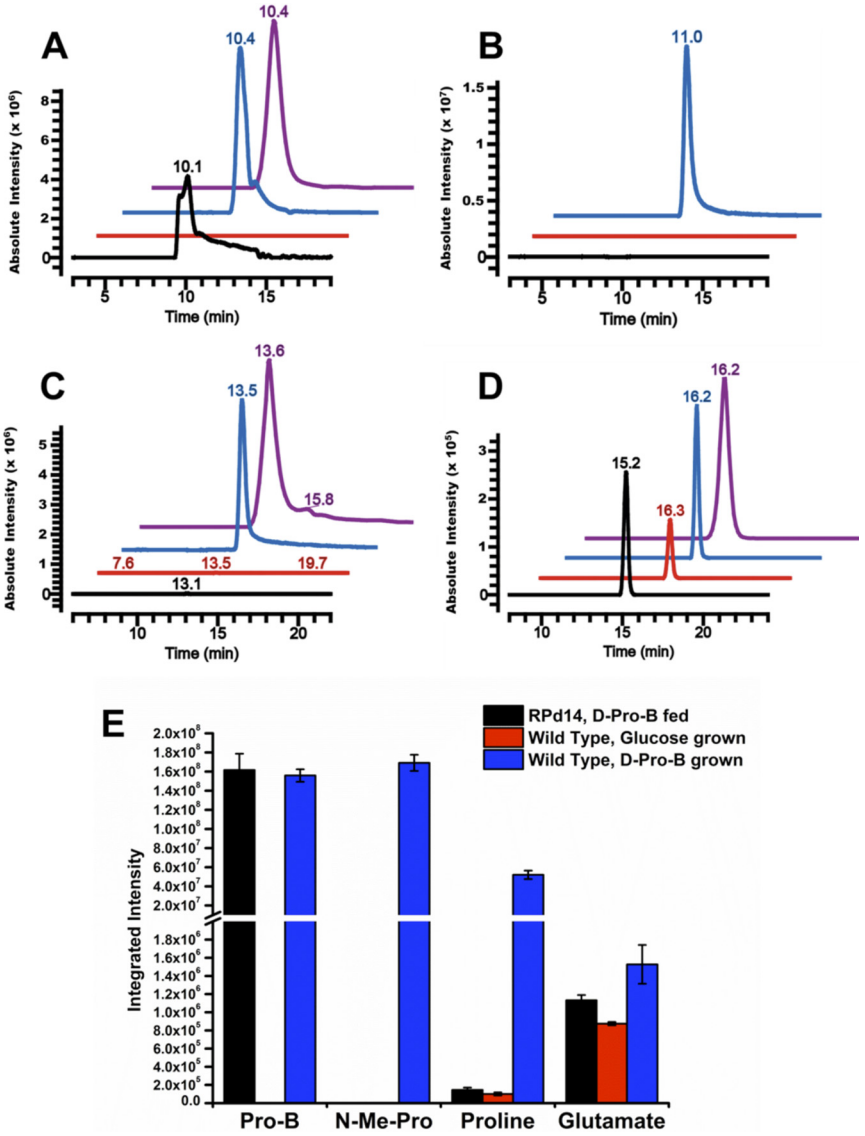

FIG 6 Accumulation of D-proline betaine catabolic metabolites measured by LC-FTMS. (A to D) Extracted ion chromatograms of representative LC-FTMS runs of extracts of the *P. denitrificans hpbD*, *hpbB1*, and *hpbC1* and *hpbB2* and *hpbC2* strain, RPd14, fed L-Pro-B for 1 h (black curves), wild-type *P. denitrificans* PD1222 grown on D-glucose (red curves), and the wild-type strain grown on L-Pro-B (blue curves) and standards (purple curves). The cells were extracted with 10 mM ammonium bicarbonate (pH 9.2)-buffered acetonitrile (Materials and Methods). Panels A to D correspond to the intensities (5-ppm mass accuracy) for proline betaine (M^+; 144.10191 Da), N-Me-Pro (M^+; 130.08626 Da), proline (M^+; 116.07060 Da), and glutamate (M^-; 148.06043 Da), respectively. (E) Averaged integrated intensities of the four peaks for the two strains, with conservation of the color coding of panels A to D. Standard errors are shown for four biological replicates (three for strain RPd14); each biological replicate value was the average of the results of three technical replicates. More details are given in >Fig. S5 in the supplemental material.

crystal. Crystallographic refinement statistics are shown in Table S1 in the supplemental material.

LC-FTMS metabolomics. Metabolomics of metabolite extracts was performed using a custom 11T LTQ-FT mass spectrometer (Thermo Fisher Scientific) with an Agilent 1200 high-pressure LC (HPLC) system equipped with a Sequant Zic-HILIC column (2.1 mm by 150 mm), along with an extraction procedure similar to that used in the previous analysis of *trans*-4-hydroxy-L-proline betaine catabolism by *P. denitrificans* (13, 31). Preparation of the biological samples required growth of four independent colonies of *P. denitrificans* in minimal medium with glucose as the carbon source before subculturing each in duplicate into minimal media with either glucose or D-proline betaine as the sole carbon source. These eight cultures were grown at 30°C with aeration to an OD_{600} of ca. 0.6 before being pelleted in a refrigerated centrifuge (4,000 × *g* for 8 min), resuspended in 1 vol of cold minimal medium lacking carbon, pelleted again, and resuspended in a small volume of cold minimal medium lacking carbon, measuring the OD_{600} again by dilution, and aliquoting normalized amounts of cells in triplicate for each of the eight cultures equal to 1 ml of an OD_{600} of 6. The cell aliquots were pelleted in 1.5-ml centrifuge tubes; the supernatant was discarded; and the cell pellets were stored at −80°C for <2 weeks prior to analysis.

Preparation of the *hpbD*, *hpbB1* and *hpbC1*, and *hpbB2* and *hpbC2* genetic disruption strain, RPd14, required growth in minimal medium with glucose as the sole carbon source, as this strain was expectedly unable

TABLE 4 Transcriptional analysis of wild-type *R. sphaeroides* 2.4.1[a]

Product category and gene	Locus tag (RSP)	Fold change in gene expression						
		L-Pro	L-Pro-B	D-Pro-B	Glucose (0.5 M NaCl)	D-Pro-B (0.5 M NaCl)	Methanol	15°C
Racemase								
hpbD	4007	1.1 ± 0.2*	9 ± 1.5	11 ± 1.5	−7 ± 1.0	3 ± 0.5	—	−2.0 ± 0.3
Demethylases								
hpbC1	3979	1.0 ± 0.2*	11 ± 1.5	9 ± 1.6	−8 ± 1.0	2.1 ± 0.5	—	−4.5 ± 0.3
hpbB1	3978	1.5 ± 0.4*	10 ± 1.0	11 ± 1.5	−5 ± 0.4	2.8 ± 0.4	—	−4.7 ± 0.5
hpbA	3861	1.4 ± 0.2*	10.5 ± 1.2	10 ± 1.0	−5 ± 0.7	2.7 ± 0.2	—	−5.5 ± 0.5
Transcription factor								
hpbR	3977	1.1 ± 0.1*	1.9 ± 0.2*	1.9 ± 0.1*	1.4 ± 0.1*	1.3 ± 0.1*	—	
Putative transporters								
hpbJ	3998	1.5 ± 0.3	8 ± 1.6	9 ± 1.5	5.5 ± 0.3	6 ± 0.6	—	
hpbI	3999	2.0 ± 0.5	7.5 ± 1.5	8 ± 1.0	4.4 ± 0.3	7 ± 1.2	—	
hpbH	4000	1.7 ± 0.7	7.5 ± 0.7	7.5 ± 0.5	3.3 ± 0.5	8.5 ± 0.9	—	
Proline catabolism								
putA	2166	3.9 ± 0.4	4.1 ± 0.5	2.5 ± 0.5	−1.1 ± 0.1*	2.1 ± 0.3	—	
Formaldehyde detoxification								
hpbK	2575	1.1 ± 0.2*	11 ± 2	9 ± 1	−1.1 ± 0.1*	7.0 ± 1.0	25 ± 3	
hpbL	2576	1.2 ± 0.3*	11 ± 3	10 ± 2	−1.1 ± 0.1*	7.5 ± 1.0	23 ± 3	

[a] The analyses were conducted as described for Table 3. *, not significant; —, not determined.

to grow with L- or D-Pro-B as the sole carbon source. RPd14 cells grown in triplicate on glucose were washed in cold minimal medium lacking carbon as described above before being resuspended in 1 vol of minimal medium with D-Pro-B as the sole carbon source. These cells were incubated at 30°C for 1 h before being prepared as described above for normalized aliquoting (1 ml of an OD_{600} of 6), pelleting, and storage at −80° C. For liquid chromatography-Fourier transform mass spectrometry-based metabolomics analysis, the cell pellets were each extracted with 0.375 ml of 10 mM ammonium bicarbonate (pH 9.2)–90% acetonitrile, buffer B, containing 1 μg/ml internal standard (acetaminophen) at room temperature. Extraction consisted of the cells being suspended in buffer B by vigorous pipetting before vortex mixing for 15 min and three rounds of centrifugation (16,000 × *g* for 5 min) and decanting the supernatant into fresh containers, all at room temperature. Each extracted sample was injected three times at 100 μl into the Zic-HILIC column preequilibrated with 100% buffer B. Buffer A consisted of water buffered by 10 mM ammonium bicarbonate (pH 9.2). Metabolites were eluted from the column onto the electrospray ion source at a 200 μl/min flow rate via the following HPLC protocol: 2 min at 100% B, a linear gradient from 100% B to 72% B over 10.5 min, a linear gradient from 72% B to 60% B over 14.5 min, another linear gradient from 60% to 100% B over 3 min, and a 15-min reequilibration at 100% B. Standards (D-Pro-B, L-proline, and L-glutamate) were diluted into buffer B before precisely following the LC-FTMS method described above. All data were collected with polarity switching, the profile mode at 50,000 resolution, and the full scan set to *m/z* 79 to 1,000. Data analysis was performed using the Qualbrowser application of the Xcalibur suite from Thermo Fisher and a 5-ppm mass accuracy cutoff. Integrated intensities from each technical replicate were normalized using the integration of the internal standard (retention time [RT] = 3.5 min).

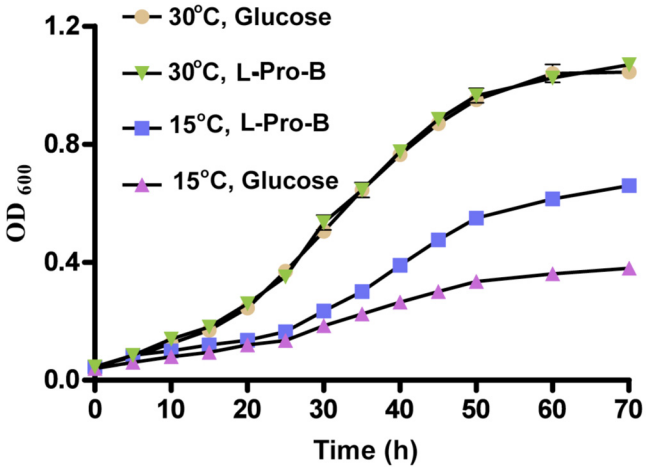

FIG 7 Effects of L-Pro-B addition on growth of wild-type *P. denitrificans* in minimal media at either 15°C or 30°C. Glucose (20 mM) was present in all cultures, whereas L-Pro-B (20 mM) was present as shown.

Bacterial strains and growth conditions. *P. denitrificans* and *R. sphaeroides* wild-type and mutant strains were grown in minimal medium containing (per liter) 6.0 g of K_2HPO_4, 4.0 g of KH_2PO_4, 0.15 g of sodium molybdate, 0.2 g of $MgS0_4{\cdot}7H_2O$, 0.04 g of $CaCl_2$, 0.001 g of $MnSO_4{\cdot}2H_2O$, and 1.1 g of $FeSO_4{\cdot}7H_2O$ with and without 1.6 g of NH_4Cl as the nitrogen source. Cultures were grown aerobically at 30°C or 15°C in mineral medium supplemented with glucose or succinate, L- or D-Pro-B, or methanol, all at 20 mM. *E. coli* strain TOP10 (Invitrogen) was used for plasmid maintenance, propagation, and cloning purposes. *E. coli* strain S17-1 was used for conjugation (32). Strains used are listed in Table S3 in the supplemental material. To study the role of L- or D-Pro-B in osmoprotection, cultures were grown in minimal medium with glucose plus or minus 0.5 M NaCl. *E. coli* cultures were grown at 37°C in LB (Luria-Bertani media). Antibiotics were used at the following concentrations (in μg ml^{-1}): kanamycin sulfate, 50; chloramphenicol, 35; sodium ampicillin, 100.

Construction of gene disruption mutant strains. Gene disruption strains were generated in *P. denitrificans* and *R. sphaeroides* by conjugation (33) or electroporation (34).

Molecular biology protocols. Chromosomal DNA was isolated from 3 to 5 ml of *P. denitrificans* or *R. sphaeroides* cells using a DNeasy blood & tissue kit (Qiagen) or a Wizard genomic DNA purification kit (Promega), respectively. Restriction enzymes, DNA polymerases, and T4 DNA ligases

were purchased from New England Biolabs, Fermentas, Invitrogen, or Promega. Plasmids were prepared from *E. coli* TOP10 cells using a Plasmid Minikit (Qiagen). Standard protocols were followed according to user's manuals provided or following methods described in reference 35.

Plasmid constructions for gene disruption, complementation, and protein overexpression. Construction of plasmids (see Table S3 in the supplemental material) for gene knockout in *P. denitrificans* was done as previously described (13). The *putA* orthologue was amplified from *P. denitrificans* genomic DNA using *Pfu* polymerase plus primers PDputAF and PDputAR (see Table S4) followed by insertion of the PCR products into pGEM T Easy vector (Promega). The resulting plasmids were then digested with NruI and ligated to a 900-bp fragment blunted-end chloramphenicol resistance (*cat*) cassette. This plasmid was then used as a PCR template with the same primers, and the products were ligated to vector pSUP202, which had been digested with EcoRI and treated with the Klenow fragment of DNA polymerase I plus the four deoxynucleoside triphosphates (dNTPs) to give the pRK14 plasmid used for gene disruption. The *R. sphaeroides hpbD* gene was amplified from genomic DNA using *Pfu* polymerase plus primers RSP4007F and RSP4007R (see Table S4) followed by insertion of the PCR products into pGEM T Easy vector (Promega). The resulting plasmids were digested with EcoRV and ligated to a 900-bp fragment blunted-end chloramphenicol resistance (*cat*) cassette. This plasmid was then used as a PCR template with the same primers, and the products were ligated to vector pSUP202 digested with EcoRI and treated with the Klenow fragment of DNA polymerase I plus the four dNTPs to give the pRRs1 plasmid used to generate the gene disruption of strain RRs1.

Expression plasmids and cloning, expression, and purification of *rs*HpbD. The PCR amplification was performed by using primers RSP4007F and RSP4007R and *R. sphaeroides* genomic DNA. The amplified product was digested with NdeI and BamHI (New England Biolabs) and then inserted into pET17b (Novagen). The recombinant plasmids were transformed into *E. coli* BL21 (DE3) cells for protein expression. Transformed cells were grown at 37°C in 4 liters of LB medium and were harvested after 24 h by centrifugation. The cells were resuspended in 100 ml of buffer containing 20 mM Tris-HCl (pH 8.0) and 5 mM $MgCl_2$. The suspension was lysed by sonication, and debris was cleared by centrifugation. The supernatant was applied to a DEAE Sepharose FF column and eluted with a linear gradient (1,600 ml) of 0 to 1 M NaCl buffered with 20 mM Tris-HCl (pH 8.0) containing 5 mM $MgCl_2$. Fractions containing the protein of interest were pooled and applied to a phenyl Sepharose 6 Fast Flow column in 1 M $(NH_4)_2SO_4$ for further purification. The protein was eluted with a linear gradient, 800 ml of 1 to 0 M $(NH_4)_2SO_4$, and the purest fractions were pooled and dialyzed against 20 mM Tris-HCl (pH 8.0) containing 5 mM $MgCl_2$.

Mass spectroscopy screening assay for *rs*HpbD on proline derivatives. Screening assays were set up with the following proline derivatives: L-Pro, D-Pro, *N*-methyl-L-Pro, L-Pro-B, 4-*trans*-(OH)-L-Pro, 4-*cis*-(OH)-D-Pro, *N*-methyl-4-*cis*-(OH)-L-Pro, L-Hyp-B-*N*-acetyl-4-*trans*-(OH)-L-Pro, glycyl-4-*trans*-(OH)-L-Pro, 3-*trans*-(OH)-L-Pro, 3-*cis*-(OH)-L-Pro, pyroglutamate, and pipecolate. Assays were performed in 200 μl D_2O containing 20 mM NH_4HCO_3, 0.1 mM substrate, and 1 μM enzyme. The reaction mixture was incubated at 30°C for 16 h and analyzed for incorporation of solvent deuterium as indicated by a +1 mass shift by electrospray ionization (ESI)-MS.

^{1}H NMR assay for *rs*HpbD activity on Pro-B and Hyp-B. ^{1}H nuclear magnetic resonance (NMR) spectra were recorded using a Varian Unity Inova 500-MHz NMR spectrometer. ^{1}H NMR data of racemization and epimerization were recorded in a D_2O-containing buffer at 30°C after 16 h of incubation to allow deuterium incorporation. A typical reaction mixture contained 10 mM substrate (L- or D-Pro-B and tHyp-B or cHyp-B), 25 mM sodium phosphate buffer (pD 8.0), and 1 μM enzyme.

Polarimetric assay for betaine racemase and epimerase activity. Betaine racemase and epimerase activity was measured at 25°C by quantitating the change of optical rotation. The assay was performed in a 50-mm-path-length cell in a total volume of 0.8 ml using a Jasco P-1010 polarimeter with an Hg 405-nm-pore-size filter. Buffer conditions for the assay were 50 mM Tris-HCl (pH 8.0) and 10 mM $MgCl_2$.

Syntheses of betaines. Betaines were synthesized by a slight modification of the published procedure (12). A typical reaction mixture for the synthesis of L-Pro-B, D-Pro-B, tHyp-B, and cHyp-B was as follows: L-proline (4.951 g, 0.043 mol) and NaOH (5.160 g, 0.129 mol) were dissolved in 50 ml of dry methanol. Methyl iodide (8.0 ml, 0.129 mol) was added to the solution, and the reaction mixture was refluxed with stirring for 6 h. An additional 3 ml of methyl iodide was added to the reaction mixture, and the reaction was allowed to proceed another 10 h. The solvent was removed by the use of a high-vacuum rotary evaporator over a 40°C bath. The light yellow solid was washed with ~2 liters of acetone and dried by lyophilization. The product yield was >95%, and each product was characterized by ^{1}H NMR (500 MHz; D_2O). The purity of the products was determined by optical activity measured by polarimetry.

Transcriptomics cell preparation. *P. denitrificans* and *R. sphaeroides* wild-type or mutant cultures were grown in 10 ml of minimal media with 20 mM glucose as the carbon source to an OD_{600} of 0.4. The cells were pelleted down by centrifugation (4,000 × *g*, 10 min, 4°C). Cell pellet was washed twice and resuspended in 10 ml of minimal media lacking a carbon source. The cultures were divided into two 5-ml samples. Glucose or succinate was added to one sample and L-proline, L- or D-Pro-B, or methanol was added to the second sample as the sole carbon source followed by aerobic growth at 30°C for 1 h prior to cell harvest. The effects of salt stress on gene expression were tested by addition of 0.5 M NaCl (final concentration) to the minimal media.

RNA sample preparation. For preparation of RNA samples, 1 to 5 ml of an actively growing *P. denitrificans* and *R. sphaeroides* culture (OD_{600} of 0.5 to 0.6) was added to 2 volumes of RNAprotect Bacteria Reagent (Qiagen). After vortex mixing for 10 s, the solution was incubated for 5 min at room temperature. The cells were pelleted by centrifugation (10,000 × *g* for 5 min at 4°C), the supernatant was decanted, and the remaining liquid was removed. RNA isolation was performed on ice using an RNeasy Minikit (Qiagen), following the protocols for bacteria given by Qiagen. RNA concentrations were determined by absorption at 260 nm, with 1 absorbance unit corresponding to 44 μg ml^{-1} RNA. Isolated RNA was analyzed by agarose gel electrophoresis and spectrophotometrically in a Nanodrop instrument (Thermo Scientific) using the ratios A_{260}/A_{280} and A_{260}/A_{230} and the A_{350}/A_{220} absorption spectra to assess sample integrity and purity. RNA preparation purity and absence of DNA were validated by agarose gel electrophoresis and control PCR reactions. The RNA preparations were stored at −80°C until use.

qRT-PCR. Reverse transcription (RT) was performed on 1 μg of total RNA by using a RevertAid H Minus First Strand cDNA synthesis kit (Fermentas) per the manufacturer's protocol. Of the cDNA, 1 μl was used in separate PCR reactions of 20 μl for each gene. Minus-RT controls were performed to test for genomic DNA contamination in each RNA sample. Primers were designed using a Universal Pro-Be library system (Roche Applied Science). The primer lengths were 21 to 27 nucleotides and had a theoretical melting temperature (T_m) of 58 to 60°C. The amplicon size ranged from 66 to 110 bp. Real-time PCR was carried out in 96-well plates using a Roche LightCycler 480 instrument. The 20-μl PCR mix was prepared by adding to 1 μl of cDNA template 2 μl of forward and reverse primers (final concentration, 150 nM each primer) and 10 μl of SYBR 2×-concentration green Master Mix (Roche). The PCR running conditions were 1 cycle at 95°C for 5 min, 40 cycles of amplification at 95°C for 15 s, and 60°C for 1 min. Subsequently, a dissociation program was applied with one cycle at 95°C for 15 s, 60°C for 1 min, and 95°C for 15 s. The efficiency of all the primers used in qRT-PCR was calculated as 97% ± 2%. The gene expression data were expressed as cross-point (Cp) values. The 16S rRNA gene was used as a reference gene. The data were analyzed by the $2^{-\Delta\Delta CT}$ (Livak) method (36). The data represent averages of the

results of five biological replicates. Primer sequences will be provided upon request.

Nucleotide sequence and atomic coordinate and structure factor accession numbers. The sequences described were submitted to GenBank under the accession numbers given in Table S2 in the supplemental material. The atomic coordinates and structure factors for unliganded *pd*HpBD and the complex of *pd*HpBD with L-Pro-B and cHyp-B have been deposited in the Protein Data Bank (PDB codes 4E8G, 4J1O, and 4IZG, respectively; http://www.pdb.org).

SUPPLEMENTAL MATERIAL

Supplemental material for this article may be found at http://mbio.asm.org/lookup/suppl/doi:10.1128/mBio.00933-13/-/DCSupplemental.

Text S1, PDF file, 0.1 MB.
Figure S1, PDF file, 0.2 MB.
Figure S2, PDF file, 0.2 MB.
Figure S3, PDF file, 0.5 MB.
Figure S4, PDF file, 0.6 MB.
Figure S5, PDF file, 0.9 MB.
Table S1, PDF file, 0.1 MB.
Table S2, PDF file, 0.1 MB.
Table S3, PDF file, 0.1 MB.
Table S4, PDF file, 0.1 MB.

ACKNOWLEDGMENTS

This research was supported by a cooperative agreement from the U.S. National Institutes of Health (U54GM093342). Use of the Advanced Photon Source at Argonne National Laboratory was supported by the U.S. Department of Energy, Office of Science, Office of Basic Energy Sciences, under contract no. DE-AC02-06CH11357.

Use of the Lilly Research Laboratories Collaborative Access Team (LRL-CAT) beamline at sector 31 of the Advanced Photon Source was provided by the operator, Eli Lilly and Company.

REFERENCES

1. **Csonka LN, Hanson AD.** 1991. Prokaryotic osmoregulation: genetics and physiology. Annu. Rev. Microbiol. **45:**569–606. http://dx.doi.org/10.1146/annurev.mi.45.100191.003033.
2. **Wood JM.** 2011. Bacterial osmoregulation: a paradigm for the study of cellular homeostasis. Annu. Rev. Microbiol. **65:**215–238. http://dx.doi.org/10.1146/annurev-micro-090110-102815.
3. **Smith LT.** 1996. Role of osmolytes in adaptation of osmotically stressed and chill-stressed *Listeria monocytogenes* grown in liquid media and on processed meat surfaces. Appl. Environ. Microbiol. **62:**3088–3093.
4. **Hoffmann T, Bremer E.** 2011. Protection of *Bacillus subtilis* against cold stress via compatible-solute acquisition. J. Bacteriol. **193:**1552–1562. http://dx.doi.org/10.1128/JB.01319-10.
5. **Hanson AD, Rathinasabapathi B, Rivoal J, Burnet M, Dillon MO, Gage DA.** 1994. Osmoprotective compounds in the Plumbaginaceae: a natural experiment in metabolic engineering of stress tolerance. Proc. Natl. Acad. Sci. U. S. A. **91:**306–310. http://dx.doi.org/10.1073/pnas.91.1.306.
6. **Blunden G, Smith BE, Irons MW, Yang MH, Roch OG, Patel AV.** 1992. Betaines and tertiary sulfonium compounds from 62 species of marine-algae. Biochem. Syst. Ecol. **20:**373–388. http://dx.doi.org/10.1016/0305-1978(92)90050-N.
7. **Trinchant JC, Boscari A, Spennato G, Van de Sype G, Le Rudulier D.** 2004. Proline betaine accumulation and metabolism in alfalfa plants under sodium chloride stress. Exploring its compartmentalization in nodules. Plant Physiol. **135:**1583–1594. http://dx.doi.org/10.1104/pp.103.037556.
8. **Goldmann A, Boivin C, Fleury V, Message B, Lecoeur L, Maille M, Tepfer D.** 1991. Betaine use by rhizosphere bacteria: genes essential for trigonelline, stachydrine, and carnitine catabolism in *Rhizobium meliloti* are located on pSym in the symbiotic region. Mol. Plant Microbe Interact. **4:**571–578. http://dx.doi.org/10.1094/MPMI-4-571.
9. **Goldmann A, Lecoeur L, Message B, Delarue M, Schoonejans E, Tepfer D.** 1994. Plasmid genes essential to the catabolism of proline betaine, or stachydrine, are also required for efficient nodulation by *Rhizobium-meliloti*. FEMS Microbiol. Lett. **115:**305–311. http://dx.doi.org/10.1111/j.1574-6968.1994.tb06655.x.
10. **Gloux K, Lerudulier D.** 1989. Transport and catabolism of proline betaine in salt-stressed *Rhizobium-meliloti*. Arch. Microbiol. **151:**143–148. http://dx.doi.org/10.1007/BF00414429.
11. **Burnet MW, Goldmann A, Message B, Drong R, El Amrani A, Loreau O, Slightom J, Tepfer D.** 2000. The stachydrine catabolism region in *Sinorhizobium meliloti* encodes a multi-enzyme complex similar to the xenobiotic degrading systems in other bacteria. Gene **244:**151–161. http://dx.doi.org/10.1016/S0378-1119(99)00554-5.
12. **Phillips DA, Sande ES, Vriezen JAC, de Bruijn FJ, Le Rudulier D, Joseph CM.** 1998. A new genetic locus in *Sinorhizobium meliloti* is involved in stachydrine utilization. Appl. Environ. Microbiol. **64:**3954–3960.
13. **Zhao S, Kumar R, Sakai A, Vetting MW, Wood BM, Brown S, Bonanno JB, Hillerich BS, Seidel RD, Babbitt PC, Almo SC, Sweedler JV, Gerlt JA, Cronan JE, Jacobson MP.** 2013. Discovery of new enzymes and metabolic pathways by using structure and genome context. Nature **502:**698–702. http://dx.doi.org/10.1038/nature12576.
14. **Nagata Y, Fukuda A, Sakai M, Iida T, Kawaguchi-Nagata K.** 2001. D-amino acid contents of mitochondria and some purple bacteria. J. Mol. Catal. B Enzym. **12:**109–113.
15. **Daughtry KD, Xiao Y, Stoner-Ma D, Cho E, Orville AM, Liu P, Allen KN.** 2012. Quaternary ammonium oxidative demethylation: X-ray crystallographic, resonance Raman, and UV-visible spectroscopic analysis of a Rieske-type demethylase. J. Am. Chem. Soc. **134:**2823–2834. http://dx.doi.org/10.1021/ja2111898.
16. **Maddocks SE, Oyston PC.** 2008. Structure and function of the LysR-type transcriptional regulator (LTTR) family proteins. Microbiology **154:**3609–3623. http://dx.doi.org/10.1099/mic.0.2008/022772-0.
17. **MacLean AM, Anstey MI, Finan TM.** 2008. Binding site determinants for the LysR-type transcriptional regulator PcaQ in the legume endosymbiont *Sinorhizobium meliloti*. J. Bacteriol. **190:**1237–1246. http://dx.doi.org/10.1128/JB.01456-07.
18. **Harms N, Reijnders WN, Koning S, van Spanning RJ.** 2001. Two-component system that regulates methanol and formaldehyde oxidation in *Paracoccus denitrificans*. J. Bacteriol. **183:**664–670. http://dx.doi.org/10.1128/JB.183.2.664-670.2001.
19. **Katoh K, Kuma K, Toh H, Miyata T.** 2005. MAFFT version 5: improvement in accuracy of multiple sequence alignment. Nucleic Acids Res. **33:**511–518. http://dx.doi.org/10.1093/nar/gki1928.
20. **Schrödi nger.** 2009. Schrödinger Suite 2009 LigPrep, version 2.3. Schrödinger, LLC, New York, NY.
21. **Friesner RA, Murphy RB, Repasky MP, Frye LL, Greenwood JR, Halgren TA, Sanschagrin PC, Mainz DT.** 2006. Extra precision glide: docking and scoring incorporating a model of hydrophobic enclosure for protein-ligand complexes. J. Med. Chem. **49:**6177–6196. http://dx.doi.org/10.1021/jm051256o.
22. **Schrödinger.** 2009. Schrödinger Suite 2009 induced fit docking protocol; Glide version 5.5, Prime version.1, Glide version 5.5, Prime version 2.1 ed. Schrödinger, LLC, New York, NY.
23. **Aslanidis C, de Jong PJ.** 1990. Ligation-independent cloning of PCR products (LIC-PCR). Nucleic Acids Res. **18:**6069–6074. http://dx.doi.org/10.1093/nar/18.20.6069.
24. **Fox BG, Blommel PG.** 2009. Autoinduction of protein expression. Curr. Protoc. Protein Sci. Chapter 5:unit 5.23. PubMed.
25. **Studier FW.** 2005. Protein production by auto-induction in high density shaking cultures. Protein Expr. Purif. **41:**207–234. http://dx.doi.org/10.1016/j.pep.2005.01.016.
26. **Leslie AG.** 2006. The integration of macromolecular diffraction data. Acta Crystallogr. D Biol. Crystallogr. **62:**48–57.
27. **Evans P.** 2006. Scaling and assessment of data quality. Acta Crystallogr. D Biol. Crystallogr. **62:**72–82. http://dx.doi.org/10.1107/S0907444905036693.
28. **McCoy AJ, Grosse-Kunstleve RW, Adams PD, Winn MD, Storoni LC, Read RJ.** 2007. Phaser crystallographic software. J. Appl. Crystallogr. **40:**658–674. http://dx.doi.org/10.1107/S0021889807021206.
29. **Zwart PH, Afonine PV, Grosse-Kunstleve RW, Hung LW, Ioerger TR, McCoy AJ, McKee E, Moriarty NW, Read RJ, Sacchettini JC, Sauter**

NK, Storoni LC, Terwilliger TC, Adams PD. 2008. Automated structure solution with the PHENIX suite. Methods Mol. Biol. **426:**419–435. http://dx.doi.org/10.1007/978-1-60327-058-8_28.

30. **Emsley P, Cowtan K.** 2004. Coot: model-building tools for molecular graphics. Acta Crystallogr. D Biol. Crystallogr. **60:**2126–2132.
31. **Erb TJ, Evans BS, Cho K, Warlick BP, Sriram J, Wood BM, Imker HJ, Sweedler JV, Tabita FR, Gerlt JA.** 2012. A RuBisCO-like protein links SAM metabolism with isoprenoid biosynthesis. Nat. Chem. Biol. **8:**926–932. http://dx.doi.org/10.1038/nchembio.1087.
32. **Simon R, Priefer U, Puhler A.** 1983. A broad host range mobilization system for in vivo genetic engineering: transposon mutagenesis in gram negative bacteria. Nat. Biotechnol. **1:**784–791. http://dx.doi.org/10.1038/nbt1183-784.
33. **Van Spanning RJ, Wansell CW, Reijnders WN, Harms N, Ras J, Oltmann LF, Stouthamer AH.** 1991. A method for introduction of unmarked mutations in the genome of *Paracoccus denitrificans*: construction of strains with multiple mutations in the genes encoding periplasmic cytochromes c550, c551i, and c553i. J. Bacteriol. **173:**6962–6970.
34. **Matsson M, Ackrell BA, Cochran B, Hederstedt L.** 1998. Carboxin resistance in *Paracoccus denitrificans* conferred by a mutation in the membrane-anchor domain of succinate:quinone reductase. Arch. Microbiol. **170:**27–37. http://dx.doi.org/10.1007/s002030050611.
35. **Sambrook J, Fritsch EF, Maniatis T.** 1989. Molecular cloning: a laboratory manual, 2nd ed. Cold Spring Harbor Laboratory Press, Cold Spring Harbor, NY.
36. **Livak KJ, Schmittgen TD.** 2001. Analysis of relative gene expression data using real-time quantitative PCR and the 2(-Delta Delta C(T)) method. Methods **25:**402–408. http://dx.doi.org/10.1006/meth.2001.1262.